

DOI: 10.1002/cphc.201300122

Photoinduced Biphasic Hydrogen Evolution: Decamethylsmocene as a Light-Driven Electron Donor

Peiyu Ge,^[a] Astrid J. Olaya,^[a] Micheál D. Scanlon,^[a] Imren Hatay Patir,^[b] Heron Vrabel,^[c] and Hubert H. Girault*^[a]*Dedicated to Professor Adam Heller*

Excitation of the weak electron donor decamethylsmocene on illumination with white light produces an excited-state species capable of reducing organically solubilized protons under biphasic conditions. Insight into the mechanism and kinetics of light-driven biphasic hydrogen evolution are obtained by analysis with gas chromatography, cyclic voltammetry, and UV/Vis and ¹H NMR spectroscopy. Formation of decamethylsmocenium hydride, which occurs prior to hydrogen evolution, is

a rapid step relative to hydrogen release and takes place independently of light activation. Remarkably, hydride formation occurs with greater efficiency (ca. 90% conversion) under biphasic conditions than when the reaction is carried out in an acidified single organic phase (ca. 20% conversion). Cyclic voltammetry studies reveal that decamethylsmocene has a higher proton affinity than either decamethylferrocene or osmocene.

1. Introduction

Photochemical water splitting or water electrolysis whereby electricity is generated from renewable sources (e.g. solar light or wind) is an attractive approach to produce molecular hydrogen (H₂).^[1–5] The “fuel”, water, can provide an almost unlimited source of protons, and the only products of the reaction are H₂ and O₂. Influential contributions to the field of solar-energy conversion leading to an explosion of productivity and development in light-driven hydrogen evolution were made by Heller.^[6,7]

The development of novel methodologies to perform the kinetically challenging hydrogen evolution reaction (HER), in which aqueous protons are reduced to H₂, is of vital technological importance for future solar-based carbon-neutral energy production.^[8–12] State-of-the-art multicomponent photocatalytic systems combine the use of 1) noble-metal-free catalysts based on first-row transition metals, such as biomimetic diiron^[13,14] or cobalt complexes (in particular the cobaloxime series),^[15–18] 2) inorganic photosensitizers, either molecular in nature or based on semiconductor particles, and 3) suitable


sacrificial electron donors. The majority of the multicomponent systems investigated initially utilized ruthenium photosensitizers in combination with noble-metal-free catalysts,^[6] which subsequently inspired the use of alternative photoactive complexes based on iridium,^[19] rhenium,^[20] or platinum^[21] centers, noble-metal-free photosensitizers (Eosin Y, Rose Bengal),^[22,23] and metalloporphyrins.^[24,25] Semiconductor-based photocatalysts and their composites may also be incorporated into such systems and are often further modified by doping, dye sensitization, or combination with smaller-bandgap semiconductors to enhance their visible-light absorption characteristics.^[26] Inspired by the light-harvesting complex in photosynthetic organisms, in which chlorophyll self-assembles to build the functional units that carry out the light-harvesting and charge-separation processes, an alternative recent approach is to develop supramolecular photocatalysts linking the light-harvesting unit to the catalytic one either by supramolecular assembly (several cobaloxime–photosensitizer complexes have been reported)^[25,27] or through covalent linkages (e.g. electronic linkage of a cobaloxime species and a ruthenium synthesizer through a TiO₂ nanoparticle).^[28] In theory, optimization of electron transfer in such supramolecular assemblies allows enhanced activity in comparison to a corresponding multicomponent system. Typical electron-donor species include ascorbic acid (AA), triethylamine (TEA), triethanolamine (TEOA), ethylenediaminetetraacetic acid (EDTA), and Na₂S/Na₂SCO₃.

The above-mentioned systems operate generally in a single aqueous or organic phase. However, it has been suggested that charge separation, the step that mainly determines the quantum yield in photochemical reactions, should be more efficient when the photoproducts of the reaction are separated in different phases, as in the light-harvesting complex of photosynthetic organisms.^[29,30] Besides fulfilling this condition, the

[a] P. Ge, A. J. Olaya, Dr. M. D. Scanlon, Prof. H. H. Girault
Laboratoire d'Electrochimie Physique et Analytique (LEPA)
Ecole Polytechnique Fédérale de Lausanne (EPFL)
Station 6, 1015 Lausanne (Switzerland)
Fax: (+41) 21-6933667
E-mail: Hubert.Girault@epfl.ch

[b] Dr. I. Hatay Patir
Department of Chemistry, Selcuk University
42031 Konya (Turkey)

[c] H. Vrabel
Laboratory of Inorganic Synthesis and Catalysis (LISC)
Ecole Polytechnique Fédérale de Lausanne (EPFL)
BCH 3305, Av. Forel 2, 1015 Lausanne (Switzerland)

 Supporting information for this article is available on the WWW under <http://dx.doi.org/10.1002/cphc.201300122>.

interface between two immiscible electrolyte solutions (ITIES)^[31–35] is recognized as a catalytic platform itself, since the separation of the reactants and products in two different phases can shift the equilibrium and thus favor the thermodynamically desirable reaction.^[30] In addition, recently it has been shown that the ITIES also provides a novel platform to develop new multicomponent or, indeed, supramolecular (i.e. the soft interface may provide a suitable environment for the interfacial self-assembly of an organically solubilized catalyst and aqueously solubilized photosensitizer or vice versa)^[36,37] catalyst systems, which may potentially be extrapolated to photochemical reactions such as hydrogen evolution.

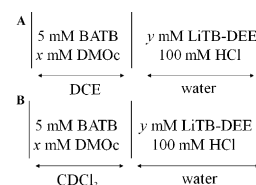
Polarization of the ITIES, either chemically (by distribution of electrolyte ions) or potentiostatically, provides an electrochemical driving force that facilitates the biphasic HER by pumping aqueous protons to an organic phase containing a suitable electron donor.^[38] Herein, we report a soluble organic sacrificial electron donor, namely, decamethylsmocene (DMOc), that is capable of proton reduction in the absence of a photosensitizer on white-light illumination under anaerobic conditions. However, decamethylsmocene remains inactive as an electron donor in the dark, that is, it combines the characteristics of both an electron donor and a sensitizer. Decamethylsmocene is one of a series of related transition metal complexes known as metallocenes, a class of hydrophobic compounds that exhibit highly reversible electrochemistry and are therefore widely used as “indicators” of potential scale in nonaqueous solvents.^[39] Among them, decamethylferrocene (DMFc; redox potential vs SHE in 1,2-dichloroethane (DCE) $[E_{\text{DMFc}^+/\text{DMFc}}^0]_{\text{SHE}}^{1,2\text{-DCE}} = 0.04 \text{ V}$)^[40] and cobaltocene (Coc) in dichloromethane (DCM) ($[E_{\text{Coc}^+/\text{Coc}}^0]_{\text{SHE}}^{\text{DCM}} = -0.69 \text{ V}$)^[41–42] are sufficiently strong reducing agents to drive the biphasic HER under anaerobic conditions in the dark. Whereas the rate of the biphasic HER is rapid with cobaltocene, it is rather slow with decamethylferrocene as electron donor and must be catalyzed by using a variety of noble (Pt, Pd)^[40] and non-noble (nanocrystalline MoS₂, MoS₂ nanoparticles grown on graphene or mesoporous carbon supports, Mo₂C, MoB, WC, W₂C)^[43–45] species. Recently, osmocene (Oc), a much weaker reducing agent ($[E_{\text{Oc}^+/\text{Oc}}^0]_{\text{SHE}}^{1,2\text{-DCE}} = 1.03 \text{ V}$), was found to split water, albeit with a low yield and low quantum efficiency, under anaerobic biphasic conditions on illumination with white light, but remained inactive as an electron donor in the dark.^[46] Thus, decamethylsmocene, with a reduction potential intermediate between that of decamethylferrocene and osmocene ($[E_{\text{DMOc}^+/\text{DMFc}}^0]_{\text{SHE}}^{1,2\text{-DCE}} = 0.48 \text{ V}$), was expected to produce quantitative amounts of H₂ on white-light illumination.

2. Results and Discussions

2.1. Shake-Flask Studies on Photoinduced Biphasic HER

2.1.1. Preliminary Experiments

The ability of DMOc to act as a light-driven organic electron donor in the biphasic HER was initially investigated by “shake-flask” reactions involving chemical polarization of the interface.^[47,48] As outlined in Scheme 1A, an aqueous solution (w)

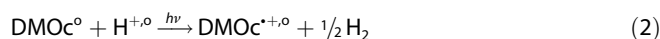


Scheme 1. Photodriven biphasic hydrogen evolution under chemical polarization: representation of the initial compositions of the aqueous and organic phases for shake-flask experiments. A) The products of the biphasic reaction, hydrogen gas and organically solubilized DMOc⁺, were monitored by gas chromatography and UV/Vis spectroscopy, respectively. B) The organic phase was additionally probed by ¹H NMR spectroscopy.

containing 100 mM HCl and 5 mM of lithium tetrakis(pentafluorophenyl)borate diethyl etherate (LiTB-DEE) was contacted with a 1,2-dichloroethane (1,2-DCE) solution containing 2.5 mM of DMOc and 5 mM of bis(triphenylphosphoranylidene) ammonium tetrakis(pentafluorophenyl)borate (BATB) with moderate stirring under white-light illumination and anaerobic conditions. The role of the tetrakis(pentafluorophenyl)borate anion (TB⁻) is to act as a phase-transfer catalyst for extraction of protons into the organic phase (o) as hydrogen tetrakis(pentafluorophenyl)borate diethyl etherate [HDEETB, referred to hereafter as HTB for simplicity; Eq. (1)]. Diethyl ether (DEE) acts as a lipophilic base.



The initial partition of the individual electrolyte ions in the biphasic system outlined in Scheme 1A established an interfacial Galvani distribution potential $\Delta_{\text{o}}^{\text{w}}\phi$ of 0.504 V for all ions at equilibrium (see the Supporting Information for details). This potential was sufficient to extract protons in the form of HTB into 1,2-DCE almost quantitatively with a concentration of 4.97 mM at equilibrium (Table S1 in the Supporting Information). The transferred protons may subsequently undergo reduction by the light-driven organic electron donor DMOc, and the reaction in Equation (2) proceeds until the supply of DMOc is exhausted:



The H₂ generated from a shake-flask experiment under white-light illumination was analyzed by gas chromatography (GC) after 120 min. An initial comparison was made between the amounts of H₂ evolved in the presence (1.7 μmol) and absence (0 μmol) of white light after 120 min (Figure 1A). The absence of H₂ evolution in the dark confirms that the standard redox potential of the ground state of DMOc in 1,2-DCE ($[E_{\text{DMOc}^+/\text{DMOc}}^0]_{\text{SHE}}^{1,2\text{-DCE}} = 0.48 \text{ V}$; see Figure S1) is insufficiently reducing to act as an electron donor for organically solubilized protons ($[E_{\text{H}^+/\text{H}_2}^0]_{\text{SHE}}^{1,2\text{-DCE}} = 0.55 \text{ V}$).^[38,49] As discussed in more detail below, an initial step in the biphasic H₂ evolution mechanism is rapid formation of decamethylsmocenium hydride [DMOc(H⁻)⁺ on contacting the acidic aqueous phase with the

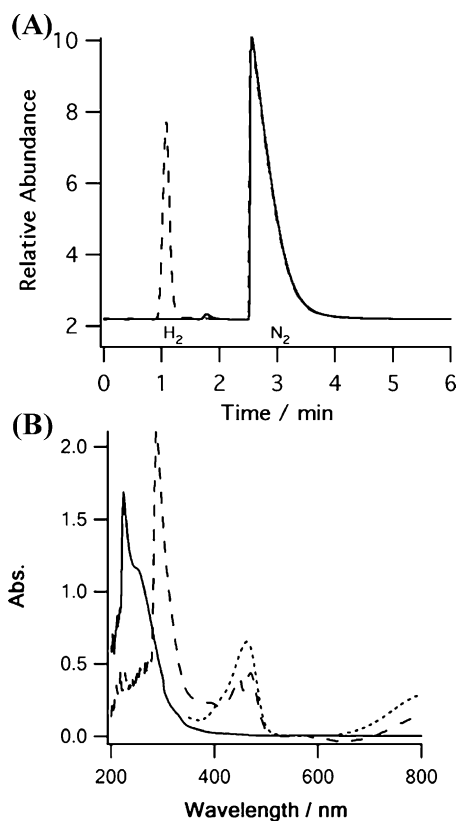


Figure 1. A) Gas chromatograms of the shake-flask headspace for two-phase reactions (see Scheme 1 A; $x=2.5$, $y=5$) after 120 min under anaerobic conditions in the dark (—) and under white-light illumination (----). B) Comparison of the UV/Vis spectra of the organic phase for two-phase reactions (see Scheme 1 A; $x=2.5$, $y=5$) before (—, showing neutral DMOc) and after (----, showing both neutral DMOc and [DMOc(H⁻)]⁺) 120 min of white-light illumination, under anaerobic conditions, with a solution of 1,2-DCE containing 2.5 mM of synthesized DMOc⁺ (••••).

organic phase, which in turn suggests that the following step of hydrogen release is the rate-limiting step. Thus, excitation of DMOc or [DMOc(H⁻)]⁺ by white light generates DMOc* or [DMOc(H⁻)]^{*+}, respectively. (Note that white light, encompassing the full spectrum of wavelengths, was utilized to ensure generation of all possible excited states, including [DMOc(H⁻)]^{*+}.) Identification of the specific excited-state species with the necessary thermodynamic driving force to reduce organic solubilized protons was outside the scope of this article. Further control experiments monitored by GC confirmed that, besides white light, each of the other constituents of the shake-flask experiments were essential to achieve the photoinduced biphasic HER. Shake-flask reactions in which either the organically solubilized electron donor (DMOc), the source of protons in the aqueous phase (i.e. carrying out experiments with neat water instead of aqueous HCl), or the polarizing molecule (LiTB-DEE) were removed, failed, in each case, to evolve H₂ (data not shown).

The light-driven biphasic HER was also evaluated by monitoring changes in the UV/Vis adsorption spectra for the conversion of organically solubilized DMOc (band centered at 243 nm, no observable absorption bands in visible region) to [DMOc(H⁻)]⁺ ($\lambda_{\max}=288$ nm) and DMOc⁺ ($\lambda_{\max}=462$ nm and

a smaller broad band centered at 798 nm, see Figure 1 B). The acquired UV/Vis spectra were unambiguously assigned to DMOc⁺ by comparison with the UV/Vis spectra of pure [DMOc⁺][BF₄⁻] crystals dissolved in 1,2-DCE (Figure 1 B).

2.1.2. Quantitative Determination of Shake-Flask Reaction Products and Kinetic Studies

The progress of the light-driven biphasic HER was first assessed by monitoring the quantities of H₂ evolved with time for the shake-flask experiments outlined in Scheme 1 A ($x=2.5$, $y=5$) by calibrated GC (Figure 2 A and B). The maximum quantity of H₂ that can be evolved is limited by the initial quantity of DMOc in 1,2-DCE and the duration of white-light illumination, which varied between 0 and 300 min. The experiments herein

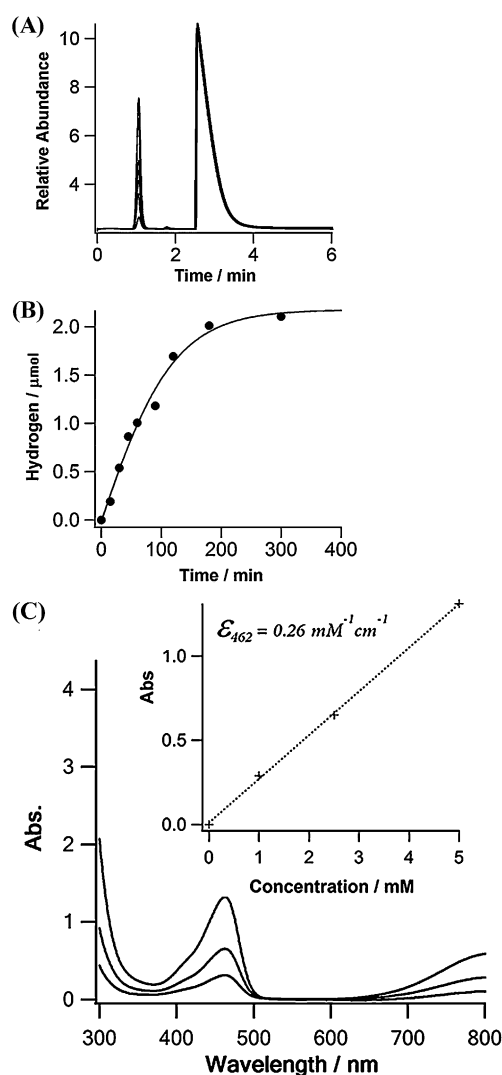
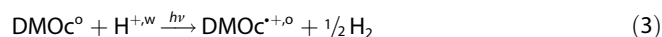


Figure 2. Quantitatively monitoring the products of the biphasic reaction, hydrogen gas and organically solubilized DMOc⁺. A) Gas chromatograms of the shake-flask headspace for two-phase reactions (see Scheme 1 (A), $x=2.5$, $y=5$), under anaerobic conditions, as a function of time and B) the resulting time course for hydrogen evolution. C) Elucidation of the molar extinction coefficient ϵ of DMOc⁺ in 1,2-DCE by plotting the absorbance (arbitrary units) versus [DMOc⁺] (inset) of the UV/Vis spectra of 1, 2.5, and 5 mM of synthesized DMOc⁺ dissolved in 1,2-DCE.

were designed with an excess of HTB, but they can be easily redesigned with HTB as the limiting factor, if required, by having a substantially greater $[\text{DMOc}^{\circ}]$ than $[\text{LiTB-DEE}^{\text{w}}]$. The quantities of H_2 evolving with time began to plateau after 180 min. (Figure 2B), and the quantity of H_2 evolved after 300 min ($2.1 \mu\text{mol}$) corresponded well with the maximum theoretical stoichiometric amount of H_2 ($2.5 \mu\text{mol}$). The theoretical amount of H_2 evolved was limited 1) by a small quantity dissolved in both phases according to Henry's equation and 2) the initial $[\text{DMOc}^{\circ}]$ ($5 \mu\text{mol}$) according to a global HER reaction with the following stoichiometry [Eq. (3)]:



The progress of the light-driven biphasic HER was also assessed by quantitative determination of the concentration of $\text{DMOc}^{+\circ}$ in the organic phase by UV/Vis spectroscopy. This was feasible by elucidation of the molar extinction coefficient ϵ of $\text{DMOc}^{+\circ}$ in 1,2-DCE as $0.26 \text{ mM}^{-1} \text{ cm}^{-1}$ for the absorption peak at $\lambda_{\text{max}} = 462 \text{ nm}$ (Figure 2C). An ϵ value of $0.11 \text{ mM}^{-1} \text{ cm}^{-1}$ was also determined for the broad peak centered at 798 nm but not used for quantitative analysis in our studies.

The ability to quantitatively determine both shake-flask reaction products, H_2 and $\text{DMOc}^{+\circ}$, permitted the application of the method of initial rates to determine the kinetics of the HER outlined in Equations (1) and (2) or globally in Equation (3). In the first instance, the initial $[\text{LiTB-DEE}^{\text{w}}]$, and hence $[\text{HTB}^{\circ}]$, was maintained constant at 5 mM and $[\text{DMOc}^{\circ}]$ was varied between 0 and 5 mM (Figure 3A). Next, the initial $[\text{DMOc}^{\circ}]$ was

kept constant at 5 mM and $[\text{LiTB-DEE}^{\text{w}}]$, and hence $[\text{HTB}^{\circ}]$, was varied between 0 and 5 mM (Figure 3B). The reaction in Equation (2) was found to be first-order in both $[\text{DMOc}^{\circ}]$ and $[\text{HTB}^{\circ}]$ with a linear dependence in the reaction velocities observed when $[\text{DMOc}^{\circ}]$ (Figure 3A) or $[\text{HTB}^{\circ}]$ (Figure 3B) was varied, irrespective of which reaction product was monitored. Thus, the rate of reaction for the light-driven biphasic HER can be written as Equation (4):

$$v = k[\text{DMOc}^{\circ}][\text{HTB}^{\circ}] \quad (4)$$

where k is the apparent rate constant for the reaction, calculated as 0.76 M min^{-1} . Also, the rate of $\text{DMOc}^{+\circ}$ formation in the organic phase was approximately twice that of H_2 evolution, and this supports the stoichiometry outlined in Equation (2). An alternative, and equally applicable, way of expressing the rate of reaction would be to consider the global reaction in Equation (3) such that [Eq. (5)]:

$$v = k[\text{DMOc}^{\circ}][\text{LiTB-DEE}^{\text{w}}] \quad (5)$$

The apparent quantum yield (AQY), defined by Equation (6),^[50] of the light reaction between DMOc and protons was determined to be 0.052% ($\lambda_{\text{irr}} = 365 \text{ nm}$, see the Supporting Information for calculations).

$$\text{AQY}/\% = \frac{\text{number of reacting electrons}}{\text{number of incident photons}} \times 100 \quad (6)$$

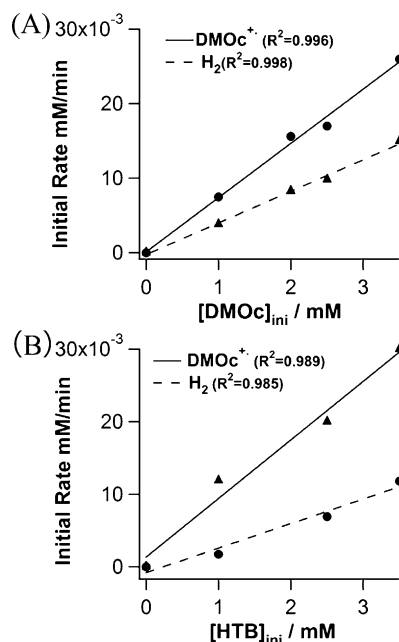
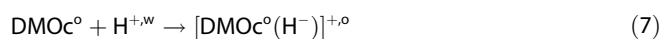


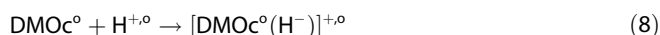
Figure 3. Kinetics of the photodriven biphasic HER with chemically controlled polarization under white-light illumination; method of initial rates. The initial rate after 60 min of illumination with white light was monitored by GC (-----) to detect evolved H_2 , and UV/Vis spectroscopy (—) to detect $\text{DMOc}^{+\circ}$ formation, whereby A) the initial $[\text{DMOc}]$ in 1,2-DCE was varied in the presence of 5 mM HTB and B) the initial $[\text{HTB}]$ was varied in the presence of 5 mM DMOc in the organic phase.

2.1.3. ^1H NMR Studies

^1H NMR spectroscopy was used as an additional probe to further elucidate the mechanism of the light-driven HER with DMOc . A freshly prepared solution of neutral DMOc in CDCl_3 containing 5 mM BATB, with no exposure to air or white-light illumination, exhibited a single peak ($\delta = 1.72 \text{ ppm}$) indicative of the protons of the methyl groups on both cyclopentadienyl rings^[51] (see Figure S2). To study the biphasic HER reaction by ^1H NMR spectroscopy, a specially designed shake-flask experiment (Scheme 1B; $x=5$, $y=5$) was required in which 1,2-DCE was replaced with CDCl_3 . On contacting the two phases for 35 min in the dark under anaerobic conditions a weak signal for unconsumed neutral DMOc ($\delta_1 = 1.75 \text{ ppm}$) and two further signals characteristic of the hydride species $[\text{DMOc}(\text{H}^-)]^+$ ($\delta_2 = 1.99 \text{ ppm}$, once more indicative of the protons of the methyl groups on both cyclopentadienyl rings, and $\delta_3 = -15.62 \text{ ppm}$, indicative of the hydride proton)^[52,53] were observed (see Figure S3). Under biphasic conditions approximately 90% DMOc was found to be converted to $[\text{DMOc}(\text{H}^-)]^+$ after 30 min. The hydride species can be formed by diffusion of organically solubilized DMOc to the interface, where it reacts with an aqueous proton [Eq. (7)]:



or by reaction of DMOc with an organically solubilized proton pumped across the interface under chemical polarization [Eqs. (2) and (8)]:



A control experiment in which the flask in Scheme 1 B was illuminated with white light, again for 30 min under anaerobic conditions, was performed, and an identical ^1H NMR spectrum showing approximately 90% conversion of DMOc to $[\text{DMOc}(\text{H}^{-})]^+$ in the organic phase was detected (Figure S4). These observations indicate that 1) hydride formation is independent of white-light illumination and 2) the protonation step under biphasic conditions is relatively fast, especially considering that completion of the global biphasic HER [Eq. (3)] under white light illumination requires up to 300 min (see Figure 2 A and B). A previous report has shown that DMOc may undergo UV photolysis under certain experimental conditions to form mono- or dications on losing protons from the cyclopentadienyl rings.^[53] However, under the biphasic experimental conditions outlined in Scheme 1 B, the lack of such signals in the ^1H NMR spectra on white-light illumination indicated the absence of any such side reactions.

Subsequently, a comparative study was performed to study hydride formation in a single phase. DMOc was dissolved in an organic phase (CDCl_3) containing both HTB and BATB, prepared as described previously.^[54] In such a scenario hydride formation can only take place by association of DMOc with organic protons. Interestingly, in the dark, protonation in a single phase proceeded much more slowly than in a biphasic system under otherwise identical experimental conditions. After 80 h approximately 20% conversion to the hydride took place, perhaps indicating a weaker acid dissociation constant in the organic phase; see Figure 4 for the time course of hydride formation. Additionally, under white-light illumination, a broad and weak peak ($\delta = 22$ ppm) was observed in the low-field region of the ^1H NMR spectrum and suggested to correspond to $\text{DMOc}^{+\circ}$ ^[55] (Figure S5).

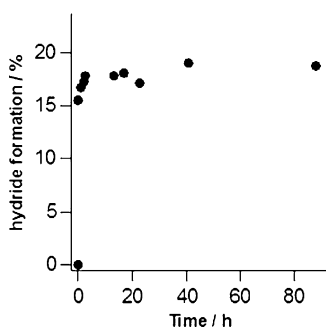
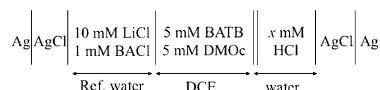


Figure 4. Time course of $[\text{DMOc}(\text{H}^{-})]^+$ formation in a one-phase system containing 5 mM DMOc and 5 mM HTB in CDCl_3 , monitored by ^1H NMR spectroscopy.

2.2. Voltammetry Studies at the Liquid | Liquid Interface

Thus far, the thermodynamic driving force pumping protons into the organic phase and enabling the biphasic HER reaction [Eq. (3)] to occur was provided by chemical distribution of common ions. Potentiostatically polarizing the interface in a four-electrode configuration (see Scheme 2 for the configuration of the electrochemical cell) may provide further insight into the mechanistic details of biphasic HER with DMOc. Figure 5 A shows cyclic voltammograms (CVs), obtained in the dark under anaerobic conditions, comparing the baseline response of the background electrolytes (no electron donor pres-



Scheme 2. Schematic representation of the composition of the electrochemical cell used for ion-transfer voltammetry.

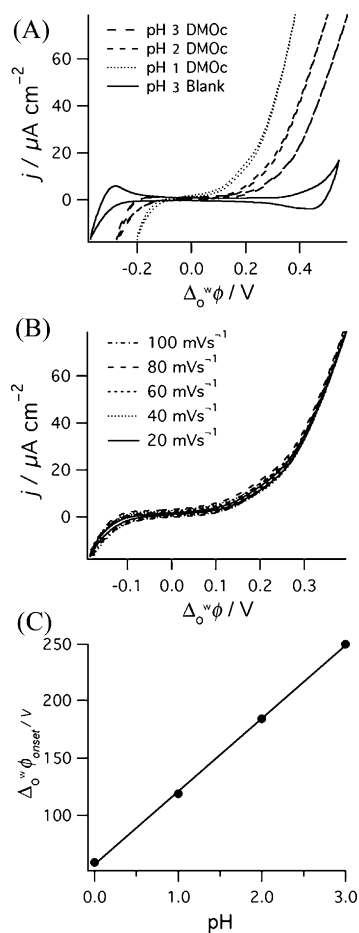


Figure 5. Ion-transfer voltammetry experiments (see electrochemical cell outlined in Scheme 2). A) Influence of pH: CV in the absence ($x=0$) and presence of DMOc ($x=5$) in the organic phase. The acidity of the aqueous phase was varied from pH 1 to 3 as indicated. CVs were obtained under anaerobic conditions at a scan rate of 20 mVs^{-1} . B) Scan rate study: CVs obtained in the presence of DMOc ($x=5$) at pH 1. C) pH dependence of $\Delta_o^w \phi_{\text{onset}}$.

ent) at pH 3 with those after addition of 5 mM DMOc to the organic phase in the pH range of 1–3. The potential window of the baseline response was limited by reversible proton and Cl⁻ transfer at the positive and negative limits, respectively. In the presence of DMOc, at each pH value, a large irreversible positive current wave dominates at positive potentials. Since organically solubilized DMOc requires photoactivation to act as an electron donor and 1) the CVs were recorded in the dark, 2) no formation of hydrogen bubbles was seen at the ITIES, and 3) ¹H NMR studies showed earlier that [DMOc(H⁻)]⁺ formation is independent of light activation, we surmise that the only reaction taking place in the dark in the electrochemical cell is the equilibrium between protonation and deprotonation of DMOc, that is, hydride formation by aqueously or organically solubilized protons. Thus, the forward-going (i.e. from negative to positive potential) current waves in Figure 5A can be attributed to the formation of [DMOc(H⁻)]⁺ with DMOc-assisted ion transfer of the proton across the interface. The absence of any observable return peaks indicates that no dissociation of the hydride species takes place when the sweep is reversed.

The Nernst equation for an assisted ion transfer at the liquid|liquid interface reads as Equation (9)^[38]:

$$\Delta_{\text{o}}^{\text{w}} \phi_{[\text{DMOc}(\text{H}^-)]^+}^{1/2} = \Delta_{\text{o}}^{\text{w}} \phi_{\text{H}^+}^{\text{o}} + \frac{RT}{2F} \ln \left(\frac{D_{\text{DMOc}}}{D_{[\text{DMOc}(\text{H}^-)]^+}} \right) - \frac{2.303 RT}{F} \text{p}K_{\text{a},[\text{DMOc}(\text{H}^-)]^+}^{1,2\text{-DCE}} + \frac{2.303 RT}{F} \text{pH}^{\text{w}} \quad (9)$$

where $\Delta_{\text{o}}^{\text{w}} \phi_{[\text{DMOc}(\text{H}^-)]^+}^{1/2}$ is the experimentally observed half-wave potential of the facilitated proton transfer, $\Delta_{\text{o}}^{\text{w}} \phi_{\text{H}^+}^{\text{o}}$ the formal transfer potential of a proton (0.55 V vs SHE),^[49] and D_{DMOc} and $D_{[\text{DMOc}(\text{H}^-)]^+}$ represent the diffusion coefficients of DMOc and [DMOc(H⁻)]⁺ in 1,2-DCE, respectively, and are assumed for simplicity to be equal, pH^w is the pH of the aqueous phase, and $\text{p}K_{\text{a},[\text{DMOc}(\text{H}^-)]^+}^{1,2\text{-DCE}}$ the $\text{p}K_{\text{a}}$ value of [DMOc(H⁻)]⁺ in 1,2-DCE. Equation (9) predicts the pH dependence of the onset potential of the irreversible wave for hydride formation, which was corroborated by the shift of the current signal by about 65 mV pH⁻¹ (Figure 5C). The $\text{p}K_{\text{a}}$ value of [DMOc(H⁻)]⁺ was estimated from Equation (9) by using the intercept of the plot in Figure 5C, and found to be 8.35. For comparison, we have previously determined the $\text{p}K_{\text{a}}$ values of [DMFc(H⁻)]⁺ and [Oc(H⁻)]⁺ to be 6.58 and 6.5, respectively, using an identical analysis.^[38,46] This means that DMOc has a higher proton affinity than DMFc or Oc ($K_{\text{a},[\text{DMOc}(\text{H}^-)]^+}^{1,2\text{-DCE}} = 4.46 \times 10^{-9}$, $K_{\text{a},[\text{DMFc}(\text{H}^-)]^+}^{1,2\text{-DCE}} = 2.63 \times 10^{-7}$, and $K_{\text{a},[\text{Oc}(\text{H}^-)]^+}^{1,2\text{-DCE}} = 3.16 \times 10^{-7}$).

Comparison of the CVs in Figure 5A with those measured previously under identical experiments conditions (in the dark, under a nitrogen atmosphere, etc.) but with replacement of DMOc with DMFc^[38] or Oc^[46] in Scheme 2 reinforce the notion that DMOc is a stronger Brønsted base than DMFc or Oc. Firstly, the higher proton affinity of DMOc means that [DMOc(H⁻)]⁺ remains undissociated during the reverse sweep and thus produces an irreversible wave. In contrast, [Oc(H⁻)]⁺ dissociates during the reverse sweep, and a reverse peak for back transfer of protons from the organic to the aqueous phase is observed.

Secondly, the current density observed for DMOc is up to five times larger than that for an equivalent concentration of DMFc in the organic phase within the same potential window. This may be due in part to the onset potential for the assisted proton transfer by DMOc $\Delta_{\text{o}}^{\text{w}} \phi_{[\text{DMOc}(\text{H}^-)]^+}^{\text{onset}}$, being more negative than that for DMFc at equivalent pH values, as indicated by Equation (9), since the $\text{p}K_{\text{a},[\text{DMOc}(\text{H}^-)]^+} > \text{p}K_{\text{a},[\text{Oc}(\text{H}^-)]^+} > \text{p}K_{\text{a},[\text{DMFc}(\text{H}^-)]^+}$. However, despite the trend in $\text{p}K_{\text{a}}$ values the current densities for DMOc and Oc are broadly similar. This reflects the fact that hydride formation (and hence the resultant current density observed) is also dependent on a host of other variables, such as the solubility of the hydride species in the respective phases. A Tafel analysis of the forward-going (i.e. from negative to positive potentials) current waves in Figure 5A was attempted and is presented in Figure S6.

A scan-rate study was performed by using the electrochemical cell described in Scheme 2 with DMOc at pH 1 (Figure 5B). The current of the irreversible wave remained independent of the applied scan rate (between 20 and 100 mVs⁻¹), and the only difference between CVs was the slightly larger capacitance at higher scan rates. Such an observation indicates that, on the timescale of the electrochemical response, the rates of diffusion of protons and DMOc to the interface are faster than their depletion at the ITIES, that is, the rate of protonation of DMOc to form the hydride species and its diffusion away from the interface.

2.3. Further Mechanistic Discussion

It is not possible to explicitly state the locus of the reaction and distinguish a heterogeneous reaction from a strictly homogeneous one under our experimental conditions. Alternative scenarios include 1) an interfacial reaction on polarization of the interface between organically solubilized DMOc and aqueous protons [see Eq. (3)] and 2) electron transfer between aqueously solubilized DMOc (even if DMOc is sparingly soluble in water) and aqueous protons [see Eqs. (10) and (11)]:



Irrespective of whether the mechanism proceeds by Equation (2), (3), or (11) or, indeed, if processes take place simultaneously, the driving force for the reaction is the same, as shown previously for the case of DMFc,^[43] and the net result is conversion of DMOc to DMOc⁺ and consumption of protons resulting in the evolution of H₂.

3. Conclusions

The above studies identified decamethylsmocene (DMOc) as a sacrificial organic electron donor that on irradiation but, notably, in the absence of a dedicated photosensitizer is capable of reducing organically solubilized protons (either pumped across the interface of a biphasic system due to the presence of a phase-transfer catalyst or present initially as an organic

acid, i.e. HTB, in a single phase) with production of hydrogen and decamethylsocenium radical cations ($\text{DMOc}^{+\cdot}$). The redox potential of the excited state of neutral DMOc or the hydride species $[\text{DMOc}(\text{H}^-)]^+$ is sufficiently negative to allow complete consumption of the sacrificial electron donor or organic acid (depending on which is limiting) and thus produce the associated quantity of hydrogen after 300 min. ^1H NMR studies revealed that conversion of DMOc to the hydride species, a key initial step leading to hydrogen evolution, occurs independently of light activation and, interestingly, with a greater efficiency under biphasic conditions than in an acidified single organic phase. The apparent quantum efficiency of the reaction ($\phi = 0.052\%$ at $\lambda_{\text{irr}} = 365$ nm) still indicates a relatively low yield for the photoproduction of hydrogen; nevertheless, it is doubled in comparison to that previously reported for a similar study in which osmocene was used as sacrificial electron donor.^[46] This work opens new perspectives, since the production of hydrogen by using light-activated weak electron donors is advantageous in so far as relatively weak electron acceptors (generated from a second half-reaction, e.g. the light-driven oxygen evolution reaction) would be required to regenerate both donor and acceptor species, thereby “resetting” the photo-system.

Experimental Section

Chemicals

All chemicals were used as received without further purification with the exception of decamethylferrocene (DMFc, $\geq 99\%$, Alfa Aesar) which was purified by vacuum sublimation at 140°C before use.^[56] All aqueous solutions were prepared with ultrapure water (Millipore Milli-Q, specific resistivity $18.2\text{ M}\Omega\text{ cm}$). The solvents used were 1,2-dichloroethane (1,2-DCE, $\geq 99.8\%$, Fluka), deuterated chloroform (CDCl_3 , $99.8 + \text{atom}\% \text{ D}$, Merck), acetonitrile (CH_3CN , $\geq 99\%$, Aldrich), diethyl ether (DEE, $\geq 99\%$, Aldrich), acetone ($\geq 99\%$, Fluka), methanol ($\geq 99\%$, Fluka), hydrochloric acid (HCl, 37% , Merck), and sulfuric acid (H_2SO_4 , 98% , Merck). Decamethylsocenium (DMOc, 99%) and ferrocene (Fc, 98%) were supplied by ABCR and Aldrich, respectively, and stored under a nitrogen atmosphere until use. Anhydrous lithium chloride (LiCl , $\geq 99\%$), anhydrous sodium sulfate (Na_2SO_4 , $\geq 99\%$), and tetraethylammonium chloride (TEACl , $\geq 98\%$) were obtained from Fluka, and silver tetrafluoroborate (AgBF_4 , $\geq 99\%$) was purchased from Aldrich.

Lithium tetrakis(pentafluorophenyl)borate diethyl etherate (LiTB-DEE, Boulder Scientific) and bis(triphenylphosphoranylidene)ammonium chloride (BACl, $\geq 98\%$, Aldrich) were used to prepare bis(triphenylphosphoranylidene)ammonium tetrakis(pentafluorophenyl)borate (BATB) by metathesis of equimolar solutions of BACl and LiTB-DEE in methanol/water (2/1 v/v). The resulting precipitate was collected by filtration, washed, and recrystallized from acetone.^[57] Decamethylsocenium tetrafluoroborate $[\text{DMOc}^{+\cdot}][\text{BF}_4^-]$ was synthesized according to O'Hare et al.^[55] First, a solution of DMOc (100 mg, 0.21 mmol) in 1,2-DCE was added dropwise to a solution of AgBF_4 (40 mg, 0.20 mmol) prepared in CH_3CN (5 mL). Immediately, a gray precipitate and green solution were formed. The solution was filtered and the solvent removed under reduced pressure. The resulting orange solid was washed with DEE (2×20 mL) and redissolved in 1,2-DCE (10 mL).

Shake-Flask Experiments

All shake flask experiments, whether characterized by GC, UV/Vis spectroscopy, or ^1H NMR analysis, were prepared using aqueous and organic solutions thoroughly degassed with nitrogen, under anaerobic conditions in a glove box purged with nitrogen, in the dark or under white-light illumination, and at an ambient temperature of $23 \pm 2^\circ\text{C}$. Anaerobic conditions were necessary to avoid competing side reactions of DMOc with oxygen, such as H_2O_2 generation, as previously demonstrated by shake-flask experiments performed in the dark in which DMFc was used as organic electron donor.^[48, 54, 58–60] Two-phase reactions were performed in a septum-sealed glass vial; 2 mL of an acidic aqueous phase containing LiTB-DEE was contacted with an equal volume of 1,2-DCE containing the lipophilic electron donor DMOc. Magnetic stirring (900 rpm) was used to emulsify the two phases for the duration of each experiment, and the cell was illuminated by white light throughout by using a Xenon lamp. The liquid|liquid interface was polarized chemically by distribution of a common ion (highly hydrophobic TB^- , initially present in the aqueous phase) across the interface. The expected reaction products from the shake flask, the precise composition of which is outlined in Scheme 1A, were H_2 and $\text{DMOc}^{+\cdot}$ [see Eq. (2)]. The presence of both was determined after the shake flask reaction.

Analysis of evolved H_2 : 1 mL samples of the headspace gas were obtained by using a lock-in syringe with a push-pull valve (SGE Analytical Sciences) in a glove box and subsequently analyzed by GC by using a PerkinElmer as chromatograph (Clarus 400, equipped with 5 \AA molecular sieves and an 80/100 mesh) with a thermal conductivity detector (TCD) and argon as a carrier gas.

Analysis of $\text{DMOc}^{+\cdot}$ formation by UV/Vis spectroscopy: After the shake-flask reaction, the mechanically emulsified phases were first allowed to settle and then the two phases were carefully separated by using a glass pipette. UV/Vis spectra of approximately 1.5 mL samples of the organic phase were measured in a glove box on an Ocean Optics CHEM2000 spectrophotometer by using a quartz cuvette with a path length of 1 cm and a volume of 4 mL, equipped with a Teflon cap to prevent evaporation of the organic phase during the analysis. The obtained UV/Vis spectra were unambiguously assigned to $\text{DMOc}^{+\cdot}$ by comparison with the UV/Vis spectra of pure $[\text{DMOc}^{+\cdot}][\text{BF}_4^-]$ dissolved in 1,2-DCE. Quantitative determination of the concentrations of organically solubilized $\text{DMOc}^{+\cdot}$ by UV/Vis spectroscopy was possible by elucidation of the molar extinction coefficient ϵ [$\text{mm}^{-1}\text{ cm}^{-1}$] of $\text{DMOc}^{+\cdot}$ in 1,2-DCE. This was calculated from the slope of a plot of absorbance [a.u.] versus $[\text{DMOc}^{+\cdot}]$ [mM] in a cuvette with a path length of 1 cm. Each point on the calibration plot was prepared by dissolution of $[\text{DMOc}^{+\cdot}][\text{BF}_4^-]$ in 1,2-DCE to ensure maximum accuracy and not using the $\text{DMOc}^{+\cdot}$ product of the biphasic reaction due to the possible presence of unconsumed DMOc after the biphasic reaction.

The apparent quantum yield ϕ was determined by illuminating a circular area of a shake flask with a mounted high-power light emitting diode (LED) from ThorLabs at $\lambda_{\text{irr}} = 365$ nm for a specific period of time, and the quantity of H_2 evolved was determined by GC.

^1H NMR analysis: The composition of the shake flask analyzed by ^1H NMR spectroscopy is outlined in Scheme 1B. The typical organic phase utilized thus far, 1,2-DCE, was replaced by CDCl_3 . BATB ($\delta_1 = 7.45$, $\delta_2 = 7.64$ ppm)^[46] was used as an internal standard. After the shake-flask reaction, the mechanically emulsified phases were first allowed to settle and then the two phases were carefully separated by using a glass pipette. ^1H NMR analysis was performed in a NMR

tube on a Bruker Biospin Avance-400 spectrometer. Chemical shifts were expressed in parts per million (ppm) relative to chloroform ($\delta = 7.28$ ppm).^[61] The presence of water ($\delta = 1.62$ ppm)^[61] was confirmed by observation of a significant decrease in the intensity of this signal on addition of anhydrous Na_2SO_4 . Two signals ($\delta_1 = 1.25$, $\delta_2 = 1.50$ ppm) were attributed to DEE,^[61] extracted into the organic phase on contacting the organic phase with the acidic aqueous phase containing LiTB-DEE.

Kinetic studies: The composition of the shake flasks used for kinetics studies is given in Scheme 1A. Experiments were performed in which the initial concentration of DMOc in 1,2-DCE was varied in the presence of 5 mM organically solubilized protons (i.e. 5 mM LiTB-DEE was dissolved in the aqueous phase resulting in the transfer of approximately 5 mM of protons to the organic phase in the form of HTB), and the initial concentration of LiTB-DEE in the aqueous phase (thus, in effect, the initial concentration of organically solubilized protons) was varied in the presence of 5 mM of DMOc in the organic phase. For each particular value of $[\text{DMOc}^\ominus]$, for example, 2.5 mM, while $[\text{LiTB-DEE}^\ominus]$ was kept constant at 5 mM, a series of individual shake flasks were prepared and each was illuminated for a different time. Hydrogen evolved from and $\text{DMOc}^{+\bullet}$ generated in each flask were analyzed quantitatively by GC and UV/Vis spectroscopy, respectively, whereby a time course curve with respect to either hydrogen or $\text{DMOc}^{+\bullet}$ was attained by plotting the amount of hydrogen or $\text{DMOc}^{+\bullet}$ against the reaction time. The initial rate was then calculated from the initial three points of the time-course curve. The same procedure as above was repeated, except that $[\text{LiTB-DEE}^\ominus]$ was varied, while $[\text{DMOc}^\ominus]$ was maintained at 5 mM to obtain the initial rates.

Electrochemical Measurements at the Liquid|Liquid Interface

Ion-transfer voltammetry experiments at the water|1,2-DCE interface were performed in a four-electrode configuration by using a PGSTAT 30 potentiostat (Metrohm, CH). Two platinum counterelectrodes were positioned in the aqueous and organic phases to supply the current. An external potential was applied by means of Ag/AgCl reference electrodes, which were connected to the aqueous and organic phases through a Luggin capillary, as illustrated previously.^[43] The Galvani potential difference across the interface Δ_ϕ^w was estimated by taking the formal ion-transfer potential of tetraethylammonium cation (TEA^+) as 0.019 V.^[62] The obtained voltammetric data were iR -compensated by using positive feedback to compensate the resistance of the cell. The area of the liquid|liquid interface was 1.53 cm². The generic composition of the four-electrode cells studied is given in Scheme 2. All voltammetry experiments were performed by using aqueous and organic phases thoroughly degassed with nitrogen, under anaerobic conditions in a glove box filled with nitrogen, in the dark, and at an ambient temperature of 23 ± 2 °C.

Acknowledgements

This work was financially supported by the Swiss National Science Foundation SNF program "Solar fuels". The authors are thankful to Professor Xile Hu and his group for useful discussions. H. Vruble acknowledges the European Research Council for funding (European Community's Seventh Framework Programme (FP7 2007-2013)/ERC grant agreement no. 257096).

Keywords: electrochemistry · hydrogen evolution reaction · interfaces · metallocenes · photochemistry

- [1] A. Heller, *Acc. Chem. Res.* **1981**, *14*, 154–162.
- [2] A. Heller, *Sol. Energy* **1982**, *29*, 153–162.
- [3] A. J. Bard, M. A. Fox, *Acc. Chem. Res.* **1995**, *28*, 141–145.
- [4] J. D. Holladay, J. Hu, D. L. King, Y. Wang, *Catal. Today* **2009**, *139*, 244–260.
- [5] T. R. Cook, D. K. Dogutan, S. Y. Reece, Y. Surendranath, T. S. Teets, D. G. Nocera, *Chem. Rev.* **2010**, *110*, 6474–6502.
- [6] E. S. Andreiadis, M. Chavarot-Kerlidou, M. Fontecave, V. Artero, *Photochem. Photobiol.* **2011**, *87*, 946–964.
- [7] W. T. Eckenhoff, R. Eisenberg, *Dalton Trans.* **2012**, *41*, 13004–13021.
- [8] J. A. Turner, *Science* **2004**, *305*, 972–974.
- [9] N. S. Lewis, D. G. Nocera, *Proc. Natl. Acad. Sci. USA* **2006**, *103*, 15729–15735.
- [10] G. W. Crabtree, M. S. Dresselhaus, *MRS Bull.* **2008**, *33*, 421–428.
- [11] A. Sartbaeva, V. L. Kuznetsov, S. A. Wells, P. P. Edwards, *Energy Environ. Sci.* **2008**, *1*, 79–85.
- [12] M. Pagliaro, A. G. Konstandopoulos, R. Ciriminna, G. Palmisano, *Energy Environ. Sci.* **2010**, *3*, 279–287.
- [13] Y. Na, M. Wang, J. Pan, P. Zhang, B. Åkermark, L. Sun, *Inorg. Chem.* **2008**, *47*, 2805–2810.
- [14] D. Streich, Y. Astuti, M. Orlandi, L. Schwartz, R. Lomoth, L. Hammarström, S. Ott, *Chem. Eur. J.* **2010**, *16*, 60–63.
- [15] J. Hawecker, J. M. Lehn, R. Ziessel, *New J. Chem.* **1983**, *7*, 271–277.
- [16] A. Fihri, V. Artero, M. Razavet, C. Baffert, W. Leibl, M. Fontecave, *Angew. Chem.* **2008**, *120*, 574–577; *Angew. Chem. Int. Ed.* **2008**, *47*, 564–567.
- [17] P. Du, J. Schneider, G. Luo, W. W. Brennessel, R. Eisenberg, *Inorg. Chem.* **2009**, *48*, 4952–4962.
- [18] V. Artero, M. Chavarot-Kerlidou, M. Fontecave, *Angew. Chem.* **2011**, *123*, 7376–7405; *Angew. Chem. Int. Ed.* **2011**, *50*, 7238–7266.
- [19] J. I. Goldsmith, W. R. Hudson, M. S. Lowry, T. H. Anderson, S. Bernhard, *J. Am. Chem. Soc.* **2005**, *127*, 7502–7510.
- [20] B. Probst, M. Guttentag, A. Rodenberg, P. Hamm, R. Alberto, *Inorg. Chem.* **2011**, *50*, 3404–3412.
- [21] P. Du, K. Knowles, R. Eisenberg, *J. Am. Chem. Soc.* **2008**, *130*, 12576–12577.
- [22] T. Lazarides, T. McCormick, P. Du, G. Luo, B. Lindley, R. Eisenberg, *J. Am. Chem. Soc.* **2009**, *131*, 9192–9194.
- [23] P. Zhang, M. Wang, J. Dong, X. Li, F. Wang, L. Wu, L. Sun, *J. Phys. Chem. C* **2010**, *114*, 15868–15874.
- [24] X. Li, M. Wang, S. Zhang, J. Pan, Y. Na, J. Liu, B. R. Åkermark, L. Sun, *J. Phys. Chem. B* **2008**, *112*, 8198–8202.
- [25] P. Zhang, M. Wang, C. Li, X. Li, J. Dong, L. Sun, *Chem. Commun.* **2010**, *46*, 8806–8808.
- [26] C.-H. Liao, C.-W. Huang, J. C. S. Wu, *Catalyst* **2012**, *2*, 490–516.
- [27] S. Jasimuddin, T. Yamada, K. Fukujū, J. Otsuki, K. Sakai, *Chem. Commun.* **2010**, *46*, 8466–8468.
- [28] F. Lakadamyali, E. Reisner, *Chem. Commun.* **2011**, *47*, 1695–1697.
- [29] D. Fraçkowiak, E. Rabinowitch, *J. Phys. Chem.* **1966**, *70*, 3012–3014.
- [30] A. G. Volkov, M. I. Gugeshashvili, D. W. Deamer, *Electrochim. Acta* **1995**, *40*, 2849–2868.
- [31] Z. Samec, *Pure Appl. Chem.* **2004**, *76*, 2147–2180.
- [32] D. W. M. Arrigan, *Anal. Lett.* **2008**, *41*, 3233–3252.
- [33] P. Vanýsek, L. B. Ramírez, *J. Chil. Chem. Soc.* **2008**, *53*, 1455–1463.
- [34] H. H. Girault in *Electroanalytical Chemistry, A Series of Advances, Vol. 23* (Eds.: A. J. Bard, C. G. Zoski), CRC Press, Boca Raton, **2010**, pp. 1–104.
- [35] Z. Samec, *Electrochim. Acta* **2012**, *84*, 21–28.
- [36] A. J. Olaya, D. Schaming, P.-F. Brevet, H. Nagatani, H.-J. Xu, M. Meyer, H. H. Girault, *Angew. Chem.* **2012**, *124*, 6553–6557; *Angew. Chem. Int. Ed.* **2012**, *51*, 6447–6451.
- [37] A. J. Olaya, D. Schaming, P.-F. Brevet, H. Nagatani, T. Zimmermann, J. Vaníček, H.-J. Xu, C. P. Gros, J.-M. Barbe, H. H. Girault, *J. Am. Chem. Soc.* **2012**, *134*, 498–506.
- [38] I. Hatay, B. Su, F. Li, R. Partovi-Nia, H. Vruble, X. Hu, M. Ersoz, H. H. Girault, *Angew. Chem.* **2009**, *121*, 5241–5244; *Angew. Chem. Int. Ed.* **2009**, *48*, 5139–5142.

- [39] I. Noviandri, K. N. Brown, D. S. Fleming, P. T. Gulyas, P. A. Lay, A. F. Masters, L. Phillips, *J. Phys. Chem. B* **1999**, *103*, 6713–6722.
- [40] J. J. Nieminen, I. Hatay, P. Ge, M. A. Méndez, L. Murtomäki, H. H. Girault, *Chem. Commun.* **2011**, *47*, 5548–5550.
- [41] U. Koelle, P. P. Infelta, M. Graetzel, *Inorg. Chem.* **1988**, *27*, 879–883.
- [42] N. G. Connelly, W. E. Geiger, *Chem. Rev.* **1996**, *96*, 877–910.
- [43] I. Hatay, P. Y. Ge, H. Vruble, X. Hu, H. H. Girault, *Energy Environ. Sci.* **2011**, *4*, 4246–4251.
- [44] P. Ge, M. D. Scanlon, P. Peljo, X. Bian, H. Vubrel, A. O'Neill, J. N. Coleman, M. Cantoni, X. Hu, K. Kontturi, B. Liu, H. H. Girault, *Chem. Commun.* **2012**, *48*, 6484–6486.
- [45] M. D. Scanlon, X. Bian, H. Vruble, V. Amstutz, K. Schenk, B. Liu, H. H. Girault, *Phys. Chem. Chem. Phys.* **2013**, *15*, 2847–2857.
- [46] P. Ge, T. K. Todorova, I. H. Patir, A. J. Olaya, H. Vruble, M. Mendez, X. Hu, C. Corminboeuf, H. H. Girault, *Proc. Natl. Acad. Sci. USA* **2012**, *109*, 11558–11563.
- [47] V. J. Cunnane, D. J. Schiffrin, C. Beltran, G. Geblewicz, T. Solomon, *J. Electroanal. Chem.* **1988**, *247*, 203–214.
- [48] B. Su, R. P. Nia, F. Li, M. Hojeij, M. Prudent, C. Corminboeuf, Z. Samec, H. H. Girault, *Angew. Chem.* **2008**, *120*, 4691–4699; *Angew. Chem. Int. Ed.* **2008**, *47*, 4675–4678.
- [49] A. Sabela, V. Mareček, Z. Samec, R. Fuoco, *Electrochim. Acta* **1992**, *37*, 231–235.
- [50] A. Kudo, Y. Miseki, *Chem. Soc. Rev.* **2009**, *38*, 253–278.
- [51] M. O. Albers, D. C. Liles, D. J. Robinson, A. Shaver, E. Singleton, M. B. Wiege, J. C. A. Boeyens, D. C. Levendis, *Organometallics* **1986**, *5*, 2321–2327.
- [52] A. A. Kamyshova, A. Z. Kreindlin, M. I. Rybinskaya, P. V. Petrovskii, *Russ. Chem. Bull.* **1999**, *48*, 581–585.
- [53] A. A. Kamyshova, A. Z. Kreindlin, M. I. Rybinskaya, P. V. Petrovskii, N. V. Kruglova, Y. A. Borisov, *Russ. Chem. Bull.* **2003**, *52*, 2424–2433.
- [54] I. Hatay, B. Su, M. A. Méndez, C. Corminboeuf, T. Khoury, C. P. Gros, M. Bourdillon, M. Meyer, J.-M. Barbe, M. Ersoz, S. Zališ, Z. Samec, H. H. Girault, *J. Am. Chem. Soc.* **2010**, *132*, 13733–13741.
- [55] D. O'Hare, J. C. Green, T. P. Chadwick, J. S. Miller, *Organometallics* **1988**, *7*, 1335–1342.
- [56] A. Zahl, R. van Eldik, M. Matsumoto, T. W. Swaddle, *Inorg. Chem.* **2003**, *42*, 3718–3722.
- [57] D. J. Fermín, H. Dung Duong, Z. Ding, P.-F. Brevet, H. H. Girault, *Phys. Chem. Chem. Phys.* **1999**, *1*, 1461–1467.
- [58] B. Su, I. Hatay, P. Y. Ge, M. Méndez, C. Corminboeuf, Z. Samec, M. Ersoz, H. H. Girault, *Chem. Commun.* **2010**, *46*, 2918–2919.
- [59] Y. Li, S. Wu, B. Su, *Chem. Eur. J.* **2012**, *18*, 7372–7376.
- [60] P. Peljo, L. Murtomäki, T. Kallio, H.-J. Xu, M. Meyer, C. P. Gros, J.-M. Barbe, H. H. Girault, K. Laasonen, K. Kontturi, *J. Am. Chem. Soc.* **2012**, *134*, 5974–5984.
- [61] H. E. Gottlieb, V. Kotlyar, A. Nudelman, *J. Org. Chem.* **1997**, *62*, 7512–7515.
- [62] T. Wandlowski, V. Mareček, Z. Samec, *Electrochim. Acta* **1990**, *35*, 1173–1175.

Received: February 4, 2013

Published online on May 17, 2013